2009

Effect of electrolytes on CO-water mass transfer

Haiyang Zhu
Iowa State University

Brent H. Shanks
Iowa State University, bshanks@iastate.edu

Theodore J. Heindel
Iowa State University, theindel@iastate.edu

Effect of electrolytes on CO-water mass transfer

Abstract
The influence of various electrolytes such as sulfate, nitrate, and chloride on CO-water mass transfer was investigated in this study. The results indicate that the enhancement in the CO-water volumetric masstransfer coefficient ranged from 1.5 to 4.7 times that of a baseline system without electrolytes, depending on electrolyte type and concentration. For those electrolytes with the same anions, copper-containing electrolytes provided stronger enhancement, whereas for those electrolytes with the same cations, sulfate-containing electrolytes showed stronger enhancement. By measuring both the CO-water volumetric mass-transfer coefficient (kLa) and the mass-transfer coefficient (kL), it was found that the electrolytes inhibit gas bubble coalescence. This leads to an increase in the gas-liquid interfacial area, resulting in CO-water mass-transfer enhancement. In contrast, when MCM41 nanoparticles with or without functionalized mercaptopropyl groups were added to water, the mass-transfer coefficient and CO-water interfacial area were both increased.

Keywords
Mechanical Engineering, baseline systems, functionalized, gas bubbles, gas liquids, interfacial areas, mass-transfer coeficients, water mass, chlorine compounds, coalescence, mass transfer

Disciplines
Biological Engineering | Chemical Engineering | Mechanical Engineering

Effect of Electrolytes on CO−Water Mass Transfer

Haiyang Zhu,[†,‡] Brent H. Shanks,[‡] and Theodore J. Heindel*[,†]

Department of Mechanical Engineering, 2025 Black Engineering Building, and Department of Chemical and Biological Engineering, 2114 Sweeney Hall, Iowa State University, Ames, Iowa 50011

The influence of various electrolytes such as sulfate, nitrate, and chloride on CO−water mass transfer was investigated in this study. The results indicate that the enhancement in the CO−water volumetric mass-transfer coefficient ranged from 1.5 to 4.7 times that of a baseline system without electrolytes, depending on electrolyte type and concentration. For those electrolytes with the same anions, copper-containing electrolytes provided stronger enhancement, whereas for those electrolytes with the same cations, sulfate-containing electrolytes showed stronger enhancement. By measuring both the CO−water volumetric mass-transfer coefficient (k_La) and the mass-transfer coefficient (k_L), it was found that the electrolytes inhibit gas bubble coalescence. This leads to an increase in the gas−liquid interfacial area, resulting in CO−water mass-transfer enhancement. In contrast, when MCM41 nanoparticles with or without functionalized mercaptopropyl groups were added to water, the mass-transfer coefficient and CO−water interfacial area were both increased.

1. Introduction

Synthesis gas (syngas) fermentation is a potential pathway to convert biomass to fuels and chemicals such as ethanol and acetic acid because of its high efficiency and low cost.[1−5] In a syngas fermentation reactor, dissolved carbon monoxide (CO) is the sole carbon source for the microorganisms to build the desired products. However, the CO solubility is very low in fermentation media, and the CO−liquid mass transfer is very slow; hence, this limits the overall product yield and becomes the rate-limiting step in syngas fermentation.[5−8] For syngas fermentation to be economically viable, the CO−water mass-transfer rate must be improved, which is the focus of this article.

Many researchers have attempted to enhance the gas−liquid mass-transfer rate by changing the reactor type or operating parameters, increasing the power input to the gas−liquid mixture, or introducing additives in the system. Ungerman and Heindel[9] investigated the influence of impeller type and operation in a stirred-tank reactor and determined the CO−water volumetric mass-transfer coefficients for a variety of schemes. The dual Rushton-type impeller scheme was found to enhance mass transfer by up to 27% compared to the standard (single) Rushton-type impeller. However, the dual Rushton-type scheme also required the most power input, which resulted in the lowest mass-transfer rate per unit power input. Others have reported the use of additives such as surfactants, alcohols, salts, and small particles in the liquid as possible methods to enhance oxygen−water mass transfer.[10−15] Olle et al.[12] reported that the oxygen−water mass-transfer rate was enhanced by a factor of approximately 600% upon addition of magnetite (Fe_3O_4) nanoparticles coated with oleic acid and a surfactant. Zuidervaart et al.[16] concluded that the oxygen−water mass-transfer rate was enhanced by up to a factor of 250% when metal sulfate electrolytes [e.g., $CuSO_4$, $FeSO_4$, $ZnSO_4$, and $Al_2(SO_4)_3$] were added to the solution. The researchers mentioned above were focused on enhancing oxygen−water mass transfer, so it is of interest as to whether those results can be extended to CO−water mass-transfer enhancement. As recently reported,[17] the CO−water mass-transfer coefficient can be enhanced by up to approximately 190% when MCM41 nanoparticles functionalized with mercaptopropyl groups are added to the system at a concentration of 0.4 wt %.

Kluytmans et al.[18] investigated the influence of electrolyte (sodium gluconate) concentration and carbon on the gas−liquid mass-transfer coefficients in a 2D slurry column. They suggested that electrolyte addition changes the surface tension, leading to smaller gas bubbles and a higher gas holdup, resulting in gas−liquid mass-transfer enhancement. Ribeiro and Mewes[19] studied the effect of electrolytes (NaCl, Na_2SO_4, and NaI) on gas holdup in bubble columns. Their results indicated that, for a given superficial gas velocity (u_G), the gas holdup is influenced by both the concentration and the chemical nature of the added electrolyte. Others have also suggested the addition of electrolytes can enhance gas−liquid mass transfer by reducing bubble coalescence.[16,20] Despite the results mentioned above, the cause of gas−liquid mass-transfer enhancement when electrolytes are added to a liquid remains inconclusive.

In the work reported herein, various electrolytes with different cations and anions were added to water in a stirred microreactor to investigate the effect of electrolyte type and concentration on the CO−water mass-transfer coefficient (k_La). This enhancement requires further understanding to improve the CO−liquid mass transfer in fermentation reactors.

2. Experimental Procedures

2.1. Materials. Manganese(II) sulfate monohydrate and cobalt(II) sulfate heptahydrate were purchased from Sigma-Aldrich; cobalt(II) nitrate was purchased from Acros Organics; manganese(II) chloride tetrahydrate, nickel(II) sulfate hexahydrate, nickel(II) nitrate hexahydrate, nickel chloride hexahydrate, cupric(II) nitrate, magnesium sulfate heptahydrate, ferrous(II) sulfate heptahydrate, and copper(II) sulfate pentahydrate were purchased from Fisher Scientific.

2.2. Determination of CO−Water Volumetric Mass-Transfer Coefficients (k_La). CO−water volumetric mass-transfer coefficients were measured in a 250-mL microreactor filled with 200 mL of nanopure water, as shown in Figure 1a. For all experiments in this work, a stir bar was agitated with a magnetic stirrer at a constant rate of 300 rpm, and the CO flow rate was held constant at 180 mL/min. The CO−water k_La

* To whom correspondence should be addressed. Fax: +1 515 294 0057. E-mail: theindel@iastate.edu.
† Department of Mechanical Engineering.
‡ Department of Chemical and Biological Engineering.

10.1021/ie8012924 CCC: $40.75
Published on Web 02/05/2009

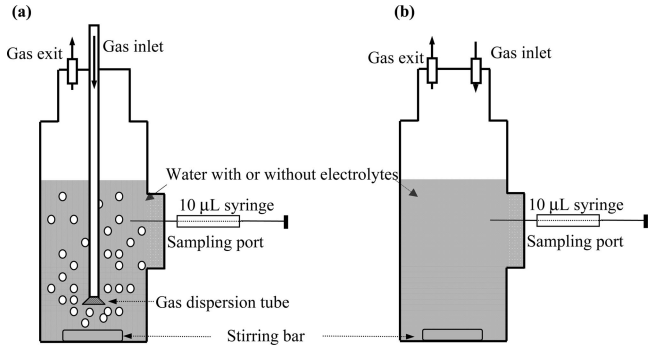

Figure 1. Schematic of the CO−water mass-transfer experimental apparatus: (a) for the enhancement in k_La and (b) for the enhancement in k_L.

values were determined by introducing a step change in CO concentration and then measuring the dissolved CO concentration as a function of time. N_2 was initially sparged through the microreactor gas inlet for ∼20 min before the gas was switched to CO. A single 10-μL liquid sample was withdrawn from the sample port using gas-tight syringes from Hamilton, and the interval between two samples was between 10 and 30 s depending on the CO−water mass-transfer rate; 13 liquid samples were collected between the CO-free and CO-saturated conditions. Dissolved CO concentrations were determined from the collected samples using a myoglobin-protein (Sigma-Aldrich) assay following the technique refined by Jones.[21] A Cary-50 Bio spectrophotometer from Varian (Mulgrave, Victoria, Australia) was used to assess the dissolved CO concentration in the liquid samples. Assuming a first-order response, the volumetric mass-transfer coefficient was then determined from the concentration data as a function of time.

The effects of various electrolytes on the CO−water volumetric mass-transfer coefficient were determined in the same vessel. The CO−water volumetric mass-transfer coefficient without electrolytes $[(k_La)_0]$ was taken as a reference before each electrolyte was added to the system. The CO−water volumetric mass-transfer coefficient with electrolytes $[(k_La)_e]$ was then determined following the procedure described above. The enhancement in CO−water mass transfer (E) was determined as

$$E = \frac{(k_La)_e}{(k_La)_0} \tag{1}$$

The effects of various electrolytes on the CO−water mass-transfer coefficient (k_L) were measured in the microreactor shown in Figure 1b, which was identical to the microreactor in Figure 1a with the exception of the gas dispersion tube. The detailed procedure was similar to the procedure described above; however, the gas−liquid mass transfer was much slower because the bulk liquid was not aerated. Hence, the interval between two liquid samples was 600 s. For this microreactor, the enhancement in the CO−water mass transfer (E) was identical to the enhancement in the CO−water mass-transfer coefficient (E_k) because the gas−liquid interfacial area (a) was constant (i.e., the gas−liquid interface was fixed because the bulk liquid was not aerated).

$$E = \frac{(k_La)_e}{(k_La)_0} = \frac{(k_L)_e}{(k_L)_0} = E_k \tag{2}$$

2.3. Error Quantification. For the reactors shown in Figure 1, the percent standard errors in k_La and k_L for each CO−water-only system were estimated to be 7.6% and 8.3%, respectively. It was assumed that the errors in the k_La and k_L were similar when electrolytes were added to the system.

3. Results and Discussion

Figure 2 shows the enhancement of CO−water volumetric mass transfer with various electrolytes as a function of electrolyte concentration. As shown in Figure 2a, the CO−water mass-transfer enhancement increased with electrolyte concentration when $CuSO_4 \cdot 5H_2O$, $CoSO_4 \cdot 7H_2O$, $NiSO_4 \cdot 7H_2O$, and $FeSO_4 \cdot 7H_2O$ were added to water. Among these electrolytes, copper sulfate showed the strongest enhancement of 4.7 when the concentration was 5 wt %. For $MnSO_4 \cdot H_2O$ and $MgSO_4 \cdot 7H_2O$, the enhancement first increased, reached a maximum, and then decreased with increasing electrolyte concentration. For the sulfate salts, the maximum enhancement differed from 3.4 to 4.7 depending on the cation type. These results suggest that, for those electrolytes with the same anion, the cation type influences the CO−liquid mass-transfer enhancement.

As shown in Figure 2b, the CO−water mass-transfer rate was enhanced upon addition of nickel electrolytes with different anions. However, the anion types showed a strong influence on the enhancement. The CO−water mass-transfer rate was enhanced by a factor of 3.9 when nickel sulfate was added to the system at a concentration of 5 wt %, whereas the CO−water mass-transfer rate was enhanced by factors of only ∼2.2 and ∼1.6, respectively, when nickel chloride or nickel nitrate were added. These results suggest that the anion type also influences the CO−water mass-transfer enhancement.

Figure 3 shows the maximum enhancements in the CO−water volumetric mass-transfer rate for various electrolytes in the concentration range of 0−5 wt %. Sulfate, chloride, and nitrate electrolytes show different enhancement ranges. When chloride and nitrate electrolytes were added to the system, the CO−water mass-transfer rates were enhanced by factors of 2.2−3.0 and 1.6−2.3, respectively, which is much smaller than the 3.4−4.7-fold enhancement for sulfate electrolytes, indicating that the sulfate anion has a stronger enhancement ability than the chloride or nitrate anion. Obviously, the anions provided a stronger influence on the mass-transfer enhancement than did the cations.

Figure 4 reveals the enhancements in the CO−water volumetric mass-transfer coefficient (E), the CO−water mass-transfer coefficient (E_k), and the calculated CO−water interface area ($E_a = E/E_k$) provided by copper sulfate as a function of electrolyte concentration. As the copper sulfate concentration increased from 0 to 5 wt %, the enhancement in CO−water volumetric mass-transfer coefficient increased from 1.0 to 4.7. In contrast, the enhancement in the CO−water mass-transfer coefficient over this same range decreased slightly from 1.1 to 0.9. As shown in Figure 4, the calculated enhancement of the CO−water interfacial area (E_a) gave a trend similar to the enhancement in CO−water volumetric mass-transfer coefficient. When the copper sulfate concentration increased from 0 to 5 wt %, the calculated enhancement in E_a increased from 1 to 5.2. Accordingly, the CO−water mass-transfer enhancement provided by the electrolytes can be concluded to have resulted from the increase in the CO−water interfacial area.

For KCl and $Ni(NO_3)_2$ samples, the CO−water mass-transfer coefficients enhancement were 0.8 and 1.0, respectively, as presented in Table 1. The CO−water mass-transfer enhancement also resulted from an increase in CO−water interfacial area. Hence, it can be concluded that the introduction of electrolytes

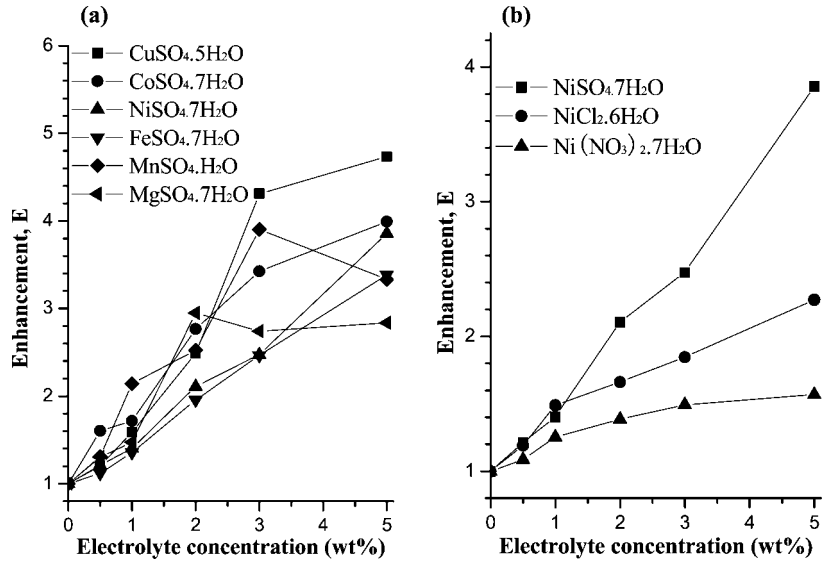

Figure 2. CO−water volumetric mass-transfer enhancement for various electrolytes as a function of electrolyte concentration: (a) sulfate electrolytes and (b) nickel electrolytes.

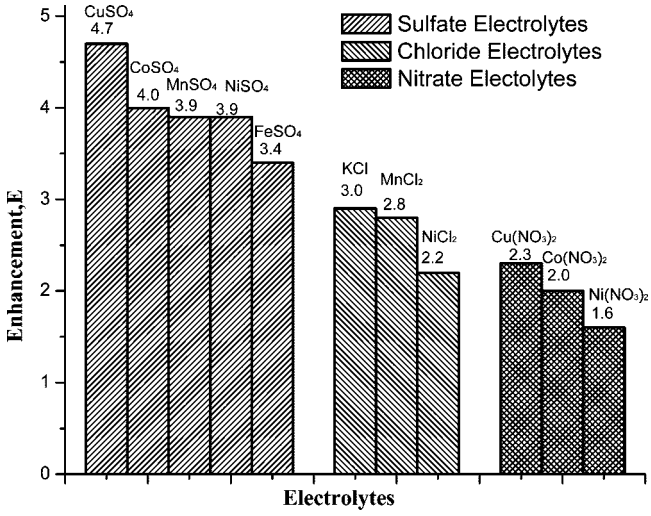

Figure 3. Maximum enhancement of CO−water volumetric mass-transfer rate for various electrolytes in a concentration range of 0−5 wt %. Note that the maximum enhancement for each electrolyte is a function of concentration.

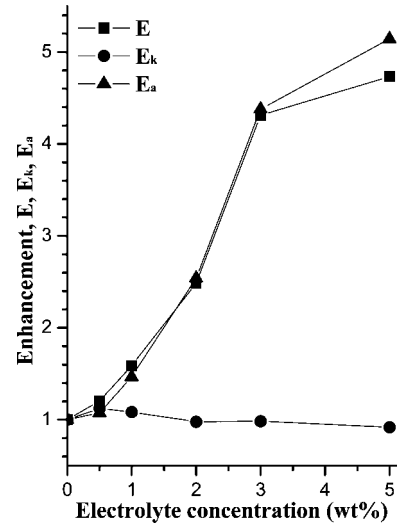

Figure 4. Enhancement in the CO−water volumetric mass-transfer coefficient (E), mass-transfer coefficient (E_k), and calculated enhancement in the CO−water interfacial area (E_a) for the copper sulfate solution as a function of copper sulfate concentration.

into the system increased the CO−water interfacial area, with this increase being a function of concentration and type.

Extending the recent results of Zhu et al.[17] for CO−water mass-transfer enhancement with nanoparticle addition, mass-transfer measurements (k_L) were determined in selected MCM41 solutions, which are also included in Table 1. For the CO−water mass-transfer enhancement upon MCM41 nanoparticle addition with and without a functionalized mercaptopropyl group at a low nanoparticle concentration of 0.4 wt %, both the CO−water mass-transfer coefficient and the CO−water interfacial area increased; this trend is different from the enhancement due to electrolyte addition. As reported previously,[17] the nanoparticles appear to adsorb CO from the gas bubbles and release it into the water; this shuttling effect results in the enhancement in the CO−water mass coefficient k_L. After functionalization by mercaptopropyl groups, the enhancement in the CO−water mass-transfer coefficient slightly increases because of the stronger CO adsorption capacity of the mercaptopropyl groups.

The enhancement due to electrolyte addition is consistent with the results reported by Kluytmans et al.,[18] who studied the

Table 1. Mass-Transfer Enhancement for Added Electrolytes and Nanoparticles

sample	enhancement		
	$E = (k_La)_e/(k_La)_0$	$E_k = (k_L)_e/(k_L)_0$	$E_a = E/E_k$
$CuSO_4$	4.7	0.9 (±0.1)	5.2
KCl	3.0	0.8	3.7
$Ni(NO_3)_2$	1.6	1.0	1.6
MCM41	1.6	1.2 (±0.1)	1.3
MPMCM41(1:19)	1.9	1.3	1.4

influence of electrolyte addition (sodium gluconate) on oxygen−liquid mass transfer in a slurry bubble column. They suggested that the enhancement resulted from the increase of the oxygen−liquid interfacial area upon addition of the electrolyte. In general, the increase in CO−water interfacial area results from a decrease of bubble size for the same volumetric flow rate, which is closely related to bubble coalescence in the reactor. Since the proposed Prince and Blanch[22] model for the rate of bubble coalescence and breakup in a gas−liquid

dispersion, several studies have been carried out to explain the bubble behavior in an electrolyte solution.

Zahradnik et al.[23] investigated the effects of electrolytes on bubble coalescence and gas holdup in bubble column reactors and concluded that gas bubble coalescence in an aqueous solution of electrolytes is significantly hindered by increasing the solute concentration. Craig et al.[20,24] used N_2, He, Ar, and SF_6 gases and $NaNO_3$, KBr, $CaCl_2$, $MgSO_4$, and NaCl electrolyte solutions to investigate the effects of electrolytes on bubble coalescence. They found that some electrolytes inhibited bubble coalescence and some electrolytes and mineral acids had no effect. They also concluded that temperature, viscosity, and surface tension had no influence on bubble coalescence.[25] Accordingly, they assigned two parameters, which they identified as α and β, to each anion and cation; the combinations $\alpha\alpha$ and $\beta\beta$ inhibited bubble coalescence, whereas the combinations $\alpha\beta$ or $\beta\alpha$ had no effect on bubble coalescence.[20,24−26] Marrucci[27] and Weissenborn and Pugh[28,29] suggested that electrolytes inhibit bubble coalescence when they increase or decrease the surface tension of water [$(d\gamma/dc)^2 > \sim 1$ mN^2, where γ is the surface tension of water and c is the concentration of electrolyte].

Others have suggested that Gibbs elasticity, which is also proportional to $(d\gamma/dc)^2$, provides an explanation for the influence of electrolytes on bubble coalescence.[30−32] Christenson and Yaminsky[31] suggested that the elastic response of the interface to changes in film thickness increases the coalescence time in electrolyte solutions compared to pure liquids (the Marangoni effect). The important quantity for this effect is the magnitude of $d\gamma/dc$ or $(d\gamma/dc)^2$. The electrolytes with low $(d\gamma/dc)^2$ values showed no inhibition in bubble coalescence.

However, Craig et al.[26] indicated that Gibbs elasticity was not the mechanism by which coalescence is inhibited; they proposed a mechanism for coalescence inhibition in which some electrolyte combinations modify the hydrodynamic conditions at the gas−liquid interface. This could account for the ion specificity in the long-range effects. Recently, Christenson et al.[33] found some electrolytes previously shown by Craig et al.[20,24−26] not to inhibit gas bubble coalescence did, in fact, inhibit coalescence at higher concentrations (>1 M). However, it is still unclear as to which mechanism(s) is (are) influenced by the presence of electrolytes during bubble coalescence because directly measuring the actual gas−liquid interfacial area in a bubble swarm in an electrolyte solution is extremely challenging.

Craig et al.[26] proposed three mechanisms whereby the short-range influence of electrolytes could control gas bubble coalescence, all of which are closely related to the change of the gas−liquid interfacial area. Accordingly, it is very helpful to explore the role of electrolytes in bubble coalescence. In the conventional view of a simple salt solution, there are no ions at the gas−liquid interface. In this case, the gas−liquid interface of an electrolyte solution should be the same as that of pure water. However, this conventional view has been challenged by recent studies[34−37] in which the anion concentration was shown to be enhanced at the gas−liquid interface. Two possible reasons were proposed to explain the anion concentration enhancement at the interface. First, water molecules at the gas−liquid interface have a preferential orientation, with the oxygen atoms pointing toward the gas. A result of this orientation is the establishment of an electric double layer at the surface. Hence, a preferential accumulation of the anions near the gas−liquid interface is expected, as the outermost portion of the double layer is negative and the innermost part is positive.[37] Second, Garrett[35] suggested that cations form hydrated clusters in which the clusters bind to the oxygen atoms in water and the water molecules are distributed symmetrically around the clusters; in contrast, the anions bind to the hydrogen atoms in water, and the water molecules are arranged asymmetrically, thus enabling water molecules to form hydrogen bonds. Hence, the cations should prefer the homogeneous environment in the liquid, whereas the anions should form asymmetric structures near the gas−liquid interface. Accordingly, the enhanced anion concentration at the gas−liquid interface would form a negative charge at the interface. This interfacial effect could influence bubble coalescence through three possible mechanisms: (i) surface tension, (ii) surface elasticity, or (iii) repulsive forces when two bubbles approach each other. Our mass-transfer results show that this influence on bubble coalescence is stronger for anions than cations and, as implied by Figure 2, is concentration-dependent.

The influence of electrolytes on bubble coalescence was also shown by Cain and Lee,[38] who investigated the drainage and rupture of the unstable film formed between two captive bubbles. They found that films formed in a 1.0 mol/L KCl solution took approximately 600 ms to drain to the rupture thickness of 55−75 nm, whereas films formed in 0.5 mol/L KCl solution took approximately 420 ms to drain and rupture at a thickness between 75 and 95 nm. However, no film could be produced between bubbles when the KCl concentration was only 0.1 mol/L. These results suggest that the films formed in the solutions with higher KCl concentrations were harder to rupture and more stable than those formed in the solutions with lower KCl concentrations, i.e., that the bubble coalescence inhibition depended on the electrolyte concentration.[38] When the KCl concentration increased, the negative charge in the double electrolyte layer at the interface increased, resulting in the suppression of bubble coalescence.

It is hypothesized that mass transfer in the presence of electrolytes is controlled by the effect(s) of electrolytes on bubble coalescence. This, in turn, is influenced by the negative charge at the interface, which depends on the anion type and concentration and modifies the resulting surface tension, surface elasticity, or repulsive force between two bubbles. An anion with a high charge or small size might be easier to accumulate at the interface, leading to a stronger influence on interfacial properties than those with low charges and large sizes. Jarvis and Scheiman[37] investigated the influence of electrolytes on surface potential and indicated that, for both sodium and magnesium electrolytes at a constant anion concentration, the surface potentials decrease in the order $SO_4^{2-} > Cl^- > NO_3^-$, which is the same as the order of CO−water mass-transfer enhancement in the present work. They also found that cations have a weaker influence on the surface tension than anions, which leads to a weaker influence on the bubble coalescence and gas−liquid mass-transfer enhancement.

Based on the discussion above, CO−water mass-transfer enhancement upon addition of electrolytes appears to result from reduced bubble coalescence. The type of electrolyte influences the results, where sulfate electrolytes provide the strongest enhancement in CO−water mass transfer, followed by chloride and nitrate electrolytes, and, in general, anions have a stronger influence than cations.

4. Conclusions

CO−water volumetric mass-transfer coefficients were found to be enhanced by a factor of up to 4.7 when electrolytes were added to nanopure water because the gas−liquid interfacial area

increased as a result of a reduction in gas bubble coalescence. The reduction in bubble coalescence was found to be closely related to electrolyte type, where anions showed a stronger influence than cations. The enhancement by MCM41 nanoparticle addition was different from that by electrolytes. The addition of MCM41 nanoparticles with or without functionalized mercaptopropyl groups led to the increase of both the CO−water mass-transfer coefficient and the CO−water interfacial area. The increase in the CO−water mass-transfer coefficient can be attributed to the shuttling effect of the MCM41 nanoparticles, i.e., MCM41 nanoparticles adsorb CO from the gas bubbles and release it into water.

Acknowledgment

This material is based on work supported by the Board of Regents, State of Iowa, through the Battelle Infrastructure and Platform Grants Program.

Literature Cited

(1) Lynd, L. R. Overview and evaluation of fuel ethanol from cellulosic biomass: Technology, economics, the environment, and policy. *Annu. Rev. Energy Environ.* **1996**, *21*, 403–465.

(2) Worden, R. M.; Bredwell, M. D.; Grethlein, A. J. Engineering issues in synthesis-gas fermentations. *Fuels Chem. Biomass* **1997**, *666*, 320–335.

(3) Ahmed, A.; Lewis, R. S. Fermentation of biomass-generated synthesis gas: Effects of nitric oxide. *Biotechnol. Bioeng.* **2007**, *97* (5), 1080–1086.

(4) Do, Y. S.; Smeenk, J.; Broer, K. M.; Kisting, C. J.; Brown, R.; Heindel, T. J.; Bobik, T. A.; DiSpirito, A. A. Growth of *Rhodospirillum rubrum* on synthesis gas: Conversion of CO to H_2 and poly-beta-hydroxyalkanoate. *Biotechnol. Bioeng.* **2007**, *97* (2), 279–286.

(5) Henstra, A. M.; Sipma, J.; Rinzema, A.; Stams, A. J. M. Microbiology of synthesis gas fermentation for biofuel production. *Curr. Opin. Biotechnol.* **2007**, *18* (3), 200–206.

(6) Vega, J. L.; Clausen, E. C.; Gaddy, J. L. Study of gaseous substrate fermentations−Carbon monoxide conversion to acetate 1. Batch culture. *Biotechnol. Bioeng.* **1989**, *34* (6), 774–784.

(7) Vega, J. L.; Antorrena, G. M.; Clausen, E. C.; Gaddy, J. L. Study of gaseous substrate fermentations−Carbon monoxide conversion to acetate 2. Continuous culture. *Biotechnol. Bioeng.* **1989**, *34* (6), 785–793.

(8) Bredwell, M. D.; Telgenhoff, M. D.; Barnard, S.; Worden, R. M. Effect of surfactants on carbon monoxide fermentations by *Butyribacterium methylotrophicum*. *Appl. Biochem. Biotechnol.* **1997**, *6* (3−5), 637–647.

(9) Ungerman, A. J.; Heindel, T. J. Carbon monoxide mass transfer for syngas fermentation in a stirred tank reactor with dual impeller configurations. *Biotechnol. Prog.* **2007**, *23* (3), 613–620.

(10) Dagaonkar, M. V.; Beenackers, A. A. C. M.; Pangarkar, V. G. Enhancement of gas−liquid mass transfer by small reactive particles at realistically high mass transfer coefficients: Absorption of sulfur dioxide into aqueous slurries of $Ca(OH)_2$ and $Mg(OH)_2$ particles. *Chem. Eng. J.* **2001**, *81* (1−3), 203–212.

(11) Py, X.; Roizard, C.; Bergault, I.; Midoux, N. Physical and chemical mass-transfer enhancement at a gas−liquid interface due to fine catalyst particles. *Chem. Eng. Res. Des.* **1995**, *73* (A3), 253–257.

(12) Olle, B.; Bucak, S.; Holmes, T. C.; Bromberg, L.; Hatton, T. A.; Wang, D. I. C. Enhancement of oxygen mass transfer using functionalized magnetic nanoparticles. *Ind. Eng. Chem. Res.* **2006**, *45* (12), 4355–4363.

(13) Hu, B.; Pacek, A. W.; Stitt, E. H.; Nienow, A. W. Bubble sizes in agitated air−alcohol systems with and without particles: Turbulent and transitional flow. *Chem. Eng. Sci.* **2005**, *60* (22), 6371–6377.

(14) El Azher, N.; Gourich, B.; Vial, C.; Bellhaj, M. S.; Bouzidi, A.; Barkaoui, M.; Ziyad, M. Influence of alcohol addition on gas hold-up, liquid circulation velocity and mass transfer coefficient in a split-rectangular airlift bioreactor. *Biochem. Eng. J.* **2005**, *23* (2), 161–167.

(15) Littlejohns, J. V.; Daugulis, A. J. Oxygen transfer in a gas−liquid system containing solids of varying oxygen affinity. *Chem. Eng. J.* **2007**, *129* (1−3), 67–74.

(16) Zuidervaart, E.; Reuter, M. A.; Heerema, R. H.; Van der Lans, R. G. J. M.; Derksen, J. J. Effect of dissolved metal sulphates on gas−liquid oxygen transfer in agitated quartz and pyrite slurries. *Min. Eng.* **2000**, *13* (14−15), 1555–1564.

(17) Zhu, H. Y.; Shanks, B. H.; Heindel, T. J. Enhancing CO−water mass transfer by functionalized MCM41 nanoparticles. *Ind. Eng. Chem. Res.* **2008**, *47* (20), 7881–7887.

(18) Kluytmans, J. H. J.; van Wachem, B. G. M.; Kuster, B. F. M.; Schouten, J. C. Mass transfer in sparged and stirred reactors: Influence of carbon particles and electrolyte. *Chem. Eng. Sci.* **2003**, *58* (20), 4719–4728.

(19) Ribeiro, C. P.; Mewes, D. The influence of electrolytes on gas hold-up and regime transition in bubble columns. *Chem. Eng. Sci.* **2007**, *62* (17), 4501–4509.

(20) Craig, V. S. J.; Ninham, B. W.; Pashley, R. M. The effect of electrolytes on bubble coalescence in water. *J. Phys. Chem.* **1993**, *97* (39), 10192–10197.

(21) Jones, S. T. Gas−liquid mass transfer in an external airlift loop reactor for syngas fermentation. Ph.D. Dissertation, Iowa State University, Ames, IA, 2007.

(22) Prince, M. J.; Blanch, H. W. Bubble coalescence and break-up in air-sparged bubble columns. *AIChE J.* **1990**, *36* (10), 1485–1499.

(23) Zahradnik, J.; Fialova, M.; Kastanek, F.; Green, K. D.; Thomas, N. H. The effect of electrolytes on bubble coalescence and gas holdup in bubble-column reactors. *Chem. Eng. Res. Des.* **1995**, *73* (A3), 341–346.

(24) Craig, V. S. J.; Ninham, B. W.; Pashley, R. M. Effect of electrolytes on bubble coalescence. *Nature* **1993**, *364* (6435), 317–319.

(25) Henry, C. L.; Dalton, C. N.; Scruton, L.; Craig, V. S. J. Ion-specific coalescence of bubbles in mixed electrolyte solutions. *J. Phys. Chem. C* **2007**, *111* (2), 1015–1023.

(26) Craig, V. S. J. Bubble coalescence and specific-ion effects. *Curr. Opin. Colloid Interface Sci.* **2004**, *9* (1−2), 178–184.

(27) Marrucci, G. A theory of coalescence. *Chem. Eng. Sci.* **1969**, *24* (6), 975.

(28) Weissenborn, P. K.; Pugh, R. J. Surface-tension and bubble coalescence phenomena of aqueous solutions of electrolytes. *Langmuir* **1995**, *11* (5), 1422–1426.

(29) Weissenborn, P. K.; Pugh, R. J. Surface tension of aqueous solutions of electrolytes: Relationship with ion hydration, oxygen solubility, and bubble coalescence. *J. Colloid Interface Sci.* **1996**, *184* (2), 550–563.

(30) Stoyanov, S. D.; Denkov, N. D. Role of surface diffusion for the drainage and hydrodynamic stability of thin liquid films. *Langmuir* **2001**, *17* (4), 1150–1156.

(31) Christenson, H. K.; Yaminsky, V. V. Solute effects on bubble coalescence. *J. Phys. Chem.* **1995**, *99* (25), 10420–10420.

(32) Hofmeier, U.; Yaminsky, V. V.; Christenson, H. K. Observations of solute effects on bubble formation. *J. Colloid Interface Sci.* **1995**, *174* (1), 199–210.

(33) Christenson, H. K.; Bowen, R. E.; Carlton, J. A.; Denne, J. R. M.; Lu, Y. Electrolytes that show a transition to bubble coalescence inhibition at high concentrations. *J. Phys. Chem. C* **2008**, *112* (3), 794–796.

(34) Creux, P.; Lachaise, J.; Graciaa, A.; Beattie, J. K. Specific cation effects at the hydroxide-charged air/water interface. *J. Phys. Chem. C* **2007**, *111* (9), 3753–3755.

(35) Garrett, B. C. Ions at the air/water interface. *Science* **2004**, *303* (5661), 1146–1147.

(36) Ghosal, S.; Hemminger, J. C.; Bluhm, H.; Mun, B. S.; Hebenstreit, E. L. D.; Ketteler, G.; Ogletree, D. F.; Requejo, F. G.; Salmeron, M. Electron spectroscopy of aqueous solution interfaces reveals surface enhancement of halides. *Science* **2005**, *307* (5709), 563–566.

(37) Jarvis, N. L.; Scheiman, M. A. Surface potentials of aqueous electrolyte solutions. *J. Phys. Chem.* **1968**, *72* (1), 74–&.

(38) Cain, F. W.; Lee, J. C. A technique for studying the drainage and rupture of unstable liquid films formed between two captive bubbles−Measurements on KCl solutions. *J. Colloid Interface Sci.* **1985**, *106* (1), 70–85.

Received for review August 25, 2008
Revised manuscript received December 29, 2008
Accepted December 31, 2008

IE8012924